SMOOTHING KINEMATIC WAVEFIELD ATTRIBUTES TO REDUCE RANDOM NOISE AND ENHANCE SIGNAL-TO-NOISE RATIO IN SEISMIC IMAGING

D. Rueda, J. H. Faccipieri, and M. Tygel

email: *dany@dep.fem.unicamp.br*

keywords: *CRS, random noise, attributes, smoothing, seismic, stack*

ABSTRACT

Signal-to-noise (S/N) ratio in seismic data is affected by random noise, influencing the continuity and identification of reflectors. In this paper, we present a method to overcome this problem based on smoothing Common-Reflection-Surface (CRS) parameters through application of local statistics in small windows aligned with reflection events. First, the CRS parameters are obtained by a standard application of the CRS stack method. Subsequently, the CRS parameters are smoothed so as to eliminate fluctuations and outliers. Finally, a CRS stack is performed with the new, smoothed parameters. The process may be iterative, to achieve an optimal result.
The proposed scheme has been applied on a 2D synthetic and a marine field data. The synthetic data application showed effective random noise attenuation plus highlighting of the reflection events. Application to the real marine data resulted in an increase of S/N ratio increases, with consequent highlight and greater continuity of the reflections.

INTRODUCTION

Random noise diminish the quality of seismic images, introducing difficulties in the identification of horizons and other image features that useful for interpretation of seismic reflection data. Uncontrolled sources, such as wind, rain, road traffic, poorly planted geophones, or electrical noise, usually generate random noise in prestack seismic data. While stacking can, at least partly, attenuate random noise in prestack data, residual random noise after stacking will still survive and affect the accuracy of final data interpretation.

Methods for random-noise attenation of seismic data is an ever present topic of interest in the literature (e. g., Yilmaz, 2001), to reduce random noise. Different methods of eliminating random noise have been developed. Bednar (1983); Duncan and Beresford (1995); Mi and Margrave (2000) incorporated median-filter noise reduction into standard Kirchhoff time migration, Gülünay (2000) used the noncausal prediction filter for random-noise attenuation, Ristau and Moon (2001) compared several adaptive filters, which they applied in an attempt to reduce random noise in geophysical data. Karsli et al. (2006) applied complex-trace analysis to seismic data for random-noise suppression, recommending it for lowfold seismic data. Transform methods were also used to eliminate seismic random noise, such as discrete cosine transform Lu and Liu (2007), curvelet transform Neelamani et al. (2008), seislet transform and seislet frame Fomel and Liu (2010).

Methods used the attenuation of random noise in seismic shot gathers sometimes leave residuals which remain in stacked seismic section decreasing the S/N ratio, leading to a decline the in the continuity of reflections and their subsequent interpretation in time or poststack depth migrations. Our idea in this work is to reduce random noise directly within the stacked seismic section, with the help of parameters obtained by the CRS stack method. The obtained CRS parameters are then subjected to smoothing process to eliminate fluctuations and outliers. Thereafter, a new CRS stack is performed using the smoothed parameters. This is an iterative process that continues up to user-selected optimal random-noise attenuation. As shown later, the procedure has been illustrated by application to a synthetic and a real marine 2D data sets, with encouraging results.

BRIEF REVIEW OF THE CRS STACK METHOD

The CRS stack method improves the S/N ratio, making use of the redundancy in seismic multicoverage data to obtain a stacked simulated zero-offset section (2D case) or volume (3D case), (see, e.g. Duveneck, 2004). For a given reference trace and time sample, $(\mathbf{x}_0, t_0)$, on the ZO (stacked) volume to be constructed, the CRS method considers the so-called generalized hyperbolic normal moveout

$$t^2\left(\Delta\mathbf{x}, \mathbf{h}\right) = \left(t_0 + \mathbf{x}^T\mathbf{a}\right)^2 + 2t_0\left(\Delta\mathbf{x}^T\mathbf{A}\Delta\mathbf{x} + \mathbf{h}^T\mathbf{B}\mathbf{h}\right), \tag{1}$$

designed to approximates the traveltimes of reflection rays in the neighborhood (paraxial) of to a reference ZO ray, which is the one that emerges at the surface point, X_0, specified on the seismic line by $\mathbf{x}_0$. The reference and paraxial rays are assumed to be primary and non-converted (PP) rays. In the above equation, $\Delta\mathbf{x}$ and $\mathbf{h}$ denote the midpoint displacement with respect to $\mathbf{x}_0$, and half-offset coordinates of the source and receiver pair, $\mathbf{x}_s$ and $\mathbf{x}_g$ in the neighborhood of $\mathbf{x}_0$. In symbols, we have

$$\Delta\mathbf{x} = \mathbf{x}_m - \mathbf{x}_0, \quad \mathbf{x}_m = \left(\mathbf{x}_g + \mathbf{x}_s\right)/2 \quad \text{and} \quad \mathbf{h} = \left(\mathbf{x}_g - \mathbf{x}_s\right)/2. \tag{2}$$

The parameters, $\mathbf{a}$, $\mathbf{A}$ and $\mathbf{B}$ and simply the coefficients of the second-order Taylor expansion of the square of traveltime in the vicinity of $(\mathbf{x}_0, t_0)$. Namely, we have

$$\mathbf{a} = \frac{\partial t}{\partial \mathbf{x}_m}, \quad \mathbf{A} = \frac{\partial^2 t}{\partial \mathbf{x}_m \mathbf{x}_m^T} \quad \text{and} \quad \mathbf{B} = \frac{\partial^2 t}{\partial \mathbf{h} \partial \mathbf{h}^T}, \tag{3}$$

all derivatives being evaluated at $\mathbf{x}_m = \mathbf{h} = \mathbf{0}$.

The linear coefficient, $\mathbf{a}$, represents the two-component vector slope at $(\mathbf{x}_0, t_0)$ of the ZO (stacked) traveltime surface to be constructed. It is related to the azimuth, α_0, and emergence angle, β_0, of the reference, ZO ray at its arrival point, X_0, at the surface. More specifically, we have

$$\mathbf{a} = \frac{2\sin\beta_0}{v_0}\begin{pmatrix} \cos\alpha_0 \\ \sin\alpha_0 \end{pmatrix}, \tag{4}$$

where v_0 is the medium (near-surface) phase velocity at X_0. Moreover, the second-order coefficients, $\mathbf{A}$ and $\mathbf{B}$ are 2×2 Hessian matrices, related to the curvature at $(\mathbf{x}_0, t_0)$ of the ZO (stacked) traveltime surface to be constructed. As described in (e.g., Duveneck, 2004), the parameters $\mathbf{A}$ and $\mathbf{B}$ can be interpreted in terms of wavefront curvature matrices, $\mathbf{K}_N$ and $\mathbf{K}_{NIP}$, of the so-called Normal (N) and Normal-Incident-Point (NIP) waves. The normal-incidence-pont, NIP, represents the point where the reference ZO ray hits the reflector. As explained in Iversen (2006), it is useful to interpret the N- and NIP-waves as related to the reference normal ray, which is the refection leg of the reference ZO ray. In other words, the reference normal way is the one that starts at the NIP, with slowness vector normal to the reflector and progresses to the surface where it emerges at the point X_0. The N-wave is then the one that starts at the NIP with identical curvature as the reflector and progresses along the reference normal way to the surface, arriving at X_0 with curvature matrix $\mathbf{K}_N$. On the other hand, the NIP-wave is the one that starts at the NIP as a point source, progresses along the reference normal ray, arriving at X_0 with curvature matrix, $\mathbf{K}_{NIP}$. More specifically, we have the relations

$$\mathbf{A} = \frac{2t_0}{v_0}\mathbf{H}^T\mathbf{K}_N\mathbf{H} \quad \text{and} \quad \mathbf{B} = \frac{2t_0}{v_0}\mathbf{H}^T\mathbf{K}_{NIP}\mathbf{H}, \tag{5}$$

in which $\mathbf{H}$ represents the transformation matrix

$$\mathbf{H} = \begin{pmatrix} \cos\alpha_0\cos\beta_0 & -\sin\alpha_0 \\ \sin\alpha_0\cos\beta_0 & \cos\alpha_0 \end{pmatrix}. \tag{6}$$

In the case of single line seismic data acquisition and 2D propagation, the vectors $\mathbf{h}$ and $\mathbf{x}_m$ reduce to scalars h and x_m. Moreover, the traveltime formula (1) the simplifies to

$$t^2(\Delta x, h) = (t_0 + ax)^2 + 2t_0\left[A(\Delta x)^2 + Bh^2\right], \tag{7}$$

with

$$a = \frac{2\sin\beta_0}{v_0}, \quad A = \frac{2t_0\cos^2\beta_0}{v_0}K_N \quad \text{and} \quad B = \frac{2t_0\cos^2\beta_0}{v_0}K_{NIP}. \tag{8}$$

in which v_0 and β_0 are as previously.

The 3D CRS operator (1), depends on eight independent parameters: the horizontal slowness (the two components of the vector, $\mathbf{a}$) and six independent components of the symmetric 2×2 matrices, $\mathbf{A}$ and $\mathbf{B}$, containing second traveltime derivatives with respect to the midpoint and offset coordinates, respectively. In the 2D case of equation (7), the number of parameters reduces to three. All parameters are determined by means of coherence analysis similar to conventional stacking velocity analysis. For each of these parameters, the results can be displayed as a 3D volume, similar to the ZO (stack) volume.

SMOOTHING OF CRS PARAMETERS

As indicated above, our methodology of random-noise attenuation is based on smoothing of CRS parameters which are obtained after a standard application of the CRS stack method. CRS parameters are estimated, in an independent way, at each sample of the stack volume to be constructed. Due to noise in the data and also on the numerics of the search procedures, the resulting parameters suffer from fluctuations along reflection events, as well as non-physical values (outliers) at points of no event. In this way, a stable parameter estimation might not be possible for every ZO location. When the CRS parameters are determined with one-parameter searches within subsets of the data, as described by (e.g., Mann et al., 1999), these searches may fail to detect the global coherency maximum for the entire CRS operator. This can also lead to outliers in the determined attributes, Duveneck (2004). Such fluctuations and outliers may have adverse effects in the stack result, and on processes such as velocity estimations that use CRS parameters. As a consequence, removing the best we can these unwanted outliers and fluctuations is a sensible thong to do.

The aplication of smoothing process to CRS sections/volumes prior to performing the final stack or using the parameters for other purposes is justified by two reasons: (a) The first- and second-order spatial traveltime derivatives which define the CRS stacking operator remain locally constant along the wavelet and (b) Under the basic assumptions of paraxial ray theory, it is expected that these spatial traveltime derivatives should vary smoothly along a reflection event.

All deviations from that expected behavior may be due to the effects of noise in the seismic data, as well as from shortcomings of the search strategy.

The smoothing algorithm applied here have been proposed, in the 2D case, by Mann and Duveneck (2004) and by Klüver and Mann (2005) for the 3D case. In both cases, the algorithm consists of constructing, for each point on the ZO (stacked) volume, taken as a candidate of a reflection, a space X time window aligned to that reflection event in the ZO stacked data volume. Once the window is constructed, local statistics (median filtering and averaging based on stack coherence and amplitudes) is applied to the set of ZO points inside the window, with the aim of returning meaningful CRS parameter values to be assigned at the window center point. In the spatial directions, the window should not exceed the first projected Fresnel zone. In order not to mix time information related to other coherent events, or valuable information with noise, the window should not be larger than the considered event wavelet. Finally, to stay inside the (candidate) reflection event, the window is tilted according to the slope of that event in the stacked section (2D case) or volume (3D case). The window slope is calculated from the angular CRS parameters at the window center, that have been estimated by the CRS stack method.

The following steps are performed for every sample in the ZO section and CRS parameter, in order to handle fluctuations as well as outliers:

- Centered around the considered ZO sample, define a smoothing window with a temporal extension of n_t samples and a spatial extension of n_x traces.

- Using the slope information (first derivatives of traveltime estimated by the angular CRS parameters) at the central ZO sample, we orient the window along the reflection event, in order to frame the reflection event.

- Reject samples below a user-defined coherence threshold in the constructed window.

- Regarding the central zero-offset sample, reject all samples in the window with dip difference θ beyond a user-defined threshold.

- Apply median filter to remove outliers.

- Apply averaging around the median to remove fluctuations.

- Assign the result to the corresponding zero-offset central sample. If there are no remaining parameters, use the original values of the ZO central sample.

- Repeat the procedure for each sample in the ZO section.

An appropriate smoothing algorithm should, in principle yield physically meaningful attribute values without destroying any relevant information, see Duveneck (2004). Only samples on the same reflection event are considered for each smoothed attribute value. There is no mixing of intersecting events due to difference of slopes in different events, conflicting dip situations need no action and do not lead to wrong results.

Remark: As well known from practical studies, the estimation of the parameters $\mathbf{a}$ and $\mathbf{B}$ is, in general, much more accurate and stable than the parameter $\mathbf{A}$. This is a consequence of the fact that the traveltime is less sensitive to that last parameter than from the first two. As a consequence, there seems to be no big loss to constrain the smoothing process to $\mathbf{a}$ and $\mathbf{B}$ only. This is what we do in the following applications.

APPLICATIONS

To demonstrate the potential of kinematic wavefield attributes smoothing in the reduction of random noise in the seismic data, we apply the method on a synthetic data set and real marine data set.

Synthetic data set

The synthetic data set was obtained by ray-tracing on the acoustic isotropic model depicted in of Figure 1. That geological model is similar to a reverse fault with an angle of $45°$ located in the central part of the model, with a few horizontal layers at both sides of the fault. The velocity field varies from 1500 to 3700 m/s, see Figure 2. The acquisition set up is that of a 2.5 model. Namely, our model is homogeneous in the y-direction (cross line), acquisition line is along the horizontal, x-direction (in-line). The acquisition geometry comprises 370 shots spaced every 40 m and 240 receivers per shot spaced every 20 m. The sampling rate is 4 ms. Random noise was added to the data with a S/N ratio of 1/100 of the largest amplitude found in the trace. Other type of noise, slash noise was added to simulate the effects of instrument problems or electrical discharges, and occur across a range of 60 traces per shot at times from 1.5 and 4.5 seconds.

The effect of the smoothing of the parameters, β_0 and K_{NIP} can be evaluated by means of the stacked sections shown in the next figures. In Figure 3 no attribute smoothing has been applied, while Figure 4 shows the stack result with smoothed attributes. In this example, a smoothing window has a temporal extension of $n_t = 2$ samples and a spatial extension of $n_x = 3$ traces. The coherence threshold was 0.005 and the maximum angle deviation allowed was $\Delta = 2°$. The stack result due to the attribute smoothing presents a significant improvement. We can see a better definition of the reflectors primarily on the location from 1 to 3 seconds, besides the amplitude of the signal corresponding to the random noise has decreased.

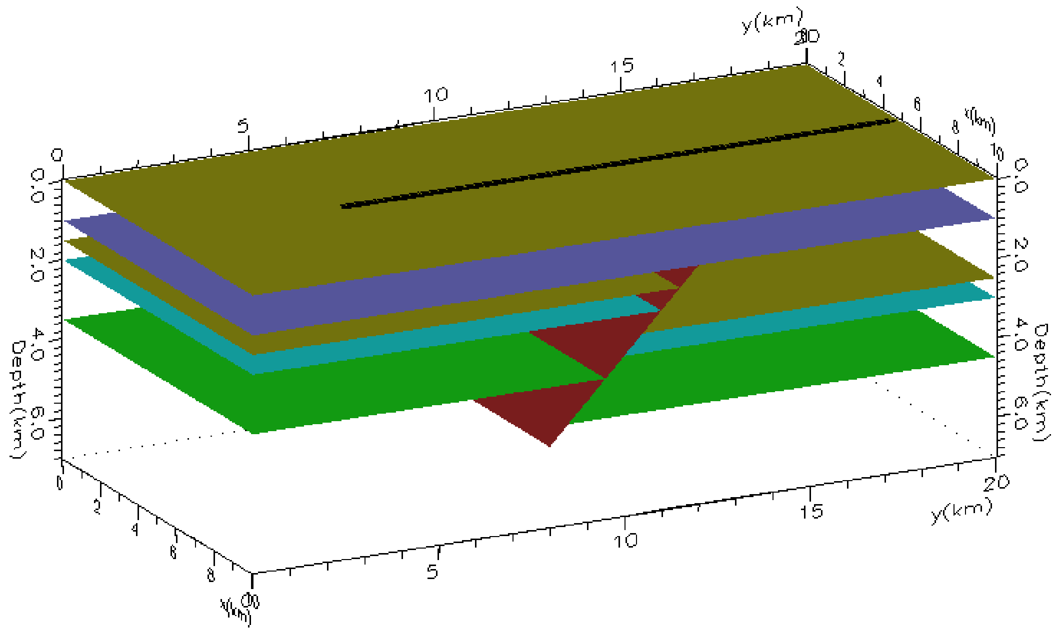

Figure 1: 2.5D model used to generate the synthetic data. Acquisition line is highlighted in black.

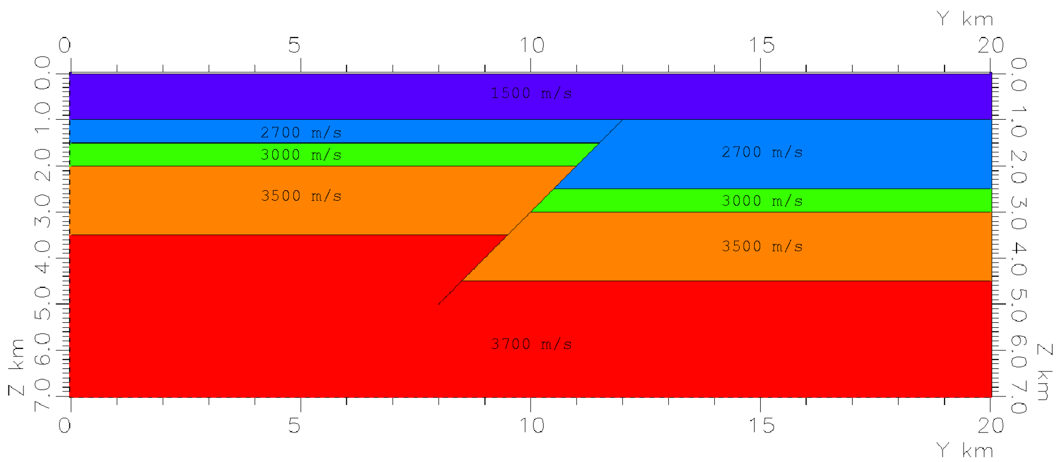

Figure 2: Velocity profile of the synthetic model.

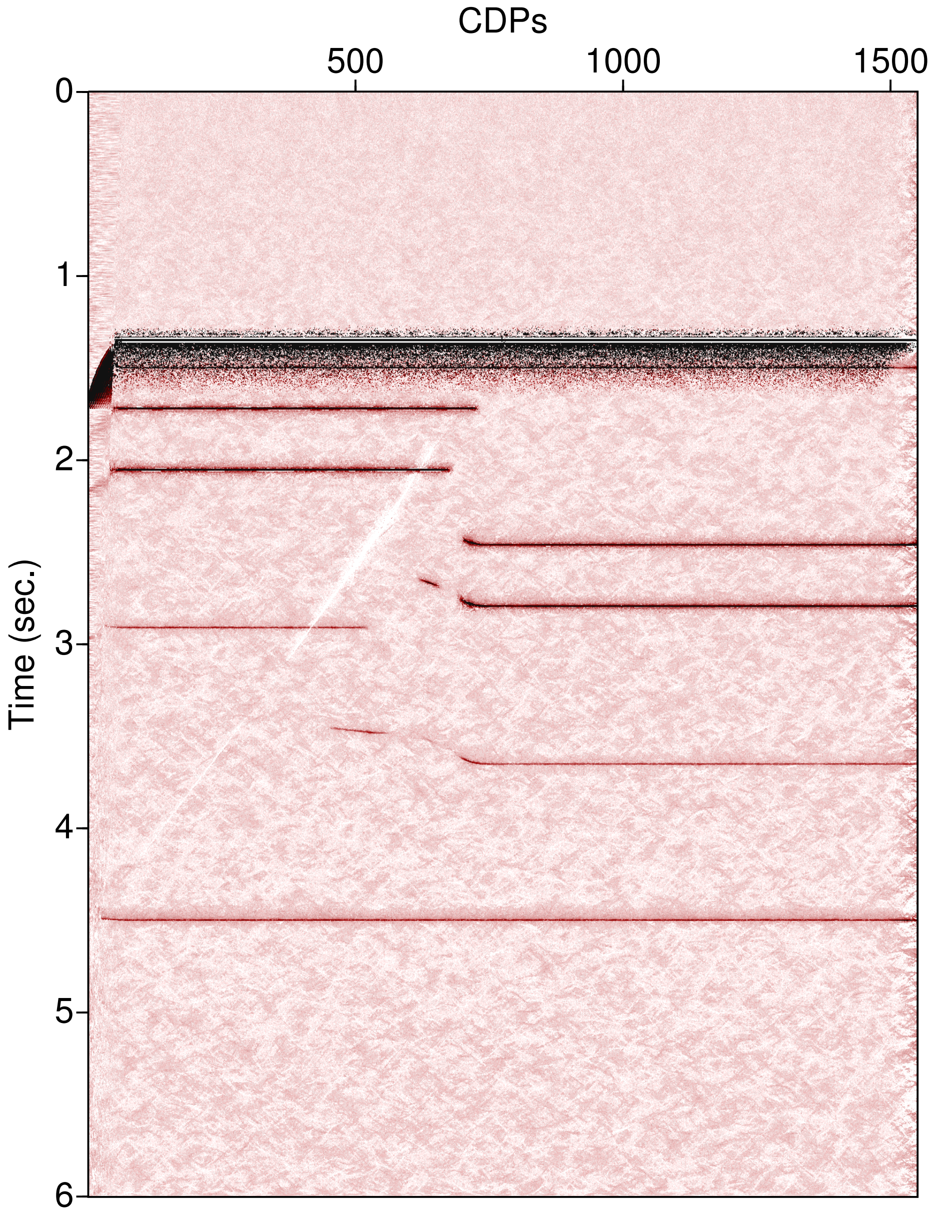

Figure 3: CRS stack result for the synthetic data set, without smoothing of β_0 and K_{NIP} sections.

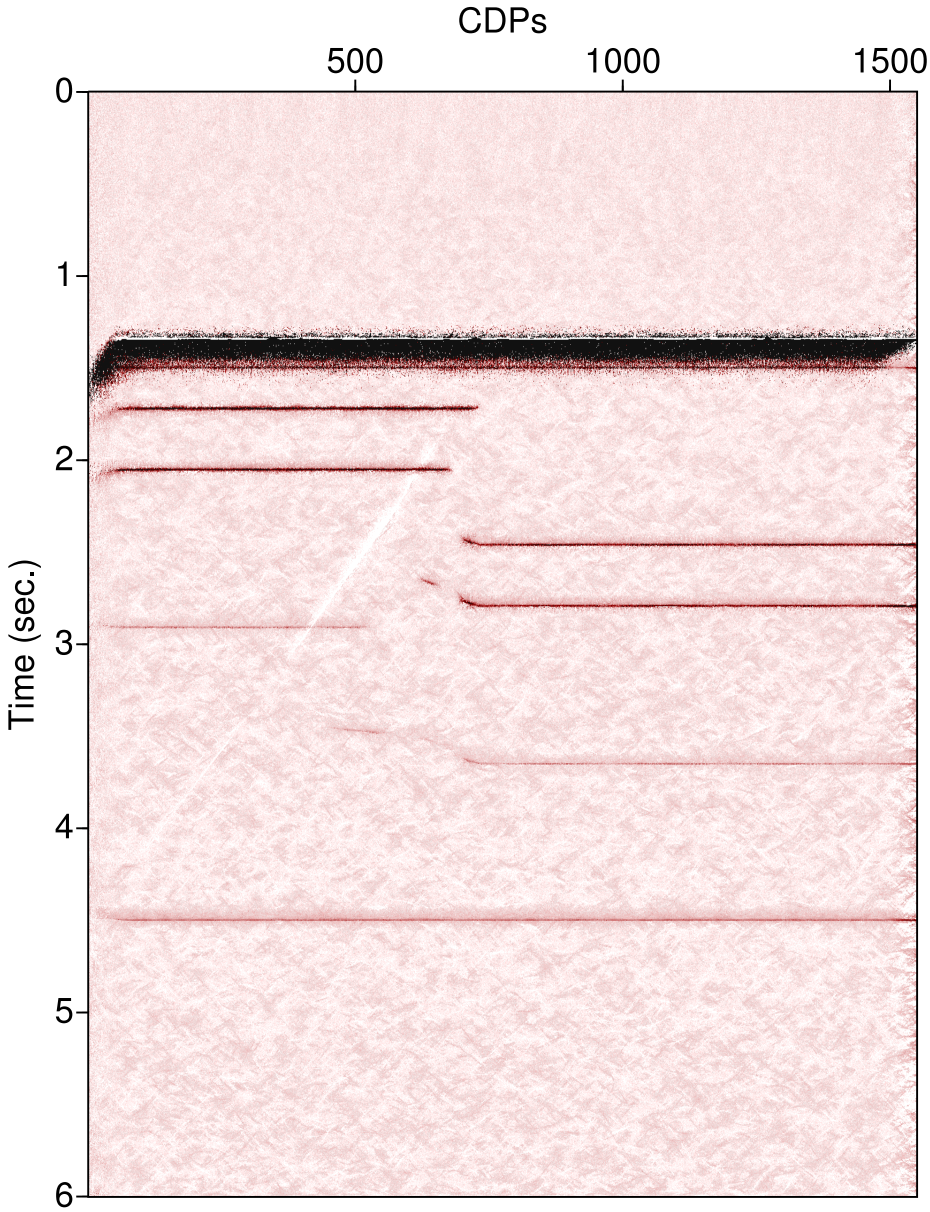

Figure 4: CRS stack result for the synthetic data set, with smoothed β_0 and K_{NIP} parameters.

Real marine data set

The same algorithm, namely smoothing of the parameters β_0 and K_{NIP} has now been applied to a real marine case. In that data set, the one-line acquisition geometry comprises 981 shots spaced every 25 m and 120 hydrophones per shot, spaced every 25 m. The sampling rate is 4 ms. The effect of the smoothing the parameters β_0 and K_{NIP} sections on the stack results can be seen in the following figures: In Figure 5, no attribute smoothing was applied, while Figure 6 shows the stack result with smoothed parameters. Figures 7 and 8 correspond to the same zoomed part of the section corresponding to Figures 5 and 6 respectively. In this example, a smoothing window has a temporal extension of $n_t = 11$ samples and a spatial extension of $n_x = 11$ traces. The coherence threshold was 0.005 and the maximum angle deviation allowed was $\Delta = 1°$. The stack result due to parameter smoothing presents a significant improvement.

CONCLUSIONS

We have presented the effectiveness of smoothing attributes to random noise attenuation and improvement of the S/N ratio in seismic data imaging. The smoothing of the kinematic wavefield attributes differentiates from others methods regarding the attenuation of ramdom noise in the stack section. The algorithm use locally valid statistics applied in small windows aligned with the reflection events. With this method is not possible to attenuate slash noise. In both synthetic data and real data, random noise attenuation was achieved.

ACKNOWLEDGMENTS

We acknowledge support from the National Council of Scientific and Technological Development (CNPq-Brazil), the National Petroleum Agency (ANP-Brazil) and the sponsors of the sponsors of the *Wave Inversion Technology (WIT) Consortium*.

REFERENCES

Bednar, J. B. (1983). Applications of median filtering to deconvolution, pulse estimation, and statistical editing of seismic data. *Geophysics*, 48:1598–1610.

Duncan, G. and Beresford, G. (1995). Some analyses of 2-D median f-k filters. *Geophysics*, 60:1157–1168.

Duveneck, E. (2004). Tomographic determination of seismic velocity models with kinematic wavefield attributes. University of Karlsruhe, logos Verlag. *Ph.D thesis*.

Fomel, S. and Liu, Y. (2010). Seislet transform and seislet frame. *Geophysics*, 25(75).

Gülünay, N. (2000). Noncausal spatial prediction filtering for random noise reduction on 3-D poststack data. *Geophysics*, 65:1641–1653.

Iversen, E. (2006). Amplitude, Fresnel zone, and NMO velocity for PP and SS normal-incidence reflections. *Geophysics*, 71:W1ŰW14.

Karsli, H., Dondurur, D., and Çifçi, G. (2006). Application of complex-trace analysis to seismic data for random-noise suppression and temporal resolution improvement. *Geophysics*, 71:V79–V86.

Klüver, T. and Mann, J. (2005). Smoothing and automated picking of kinematic wavefield attributes. In *Expanded Abstracts, 75th Ann. Internat. Mtg.*, pages 1894–1897. Soc. Expl. Geophys.

Lu, W. and Liu, J. (2007). Random noise suppression based on discrete cosine transform. In *Expanded Abstracts, 77th Ann. Internat. Mtg.*, pages 2668–2672. Soc. Expl. Geophys.

Mann, J. and Duveneck, E. (2004). Event-consistent smoothing in generalized high-density velocity analysis. In *Expanded Abstracts, 74th Ann. Internat. Mtg.* Soc. Expl. Geophys. Session ST 1.1.

Mann, J., Jäger, R., Müller, T., Höcht, G., and Hubral, P. (1999). Common-reflection-surface stack - a real data example. *J. Appl. Geoph.*, 42(3,4):283–300.

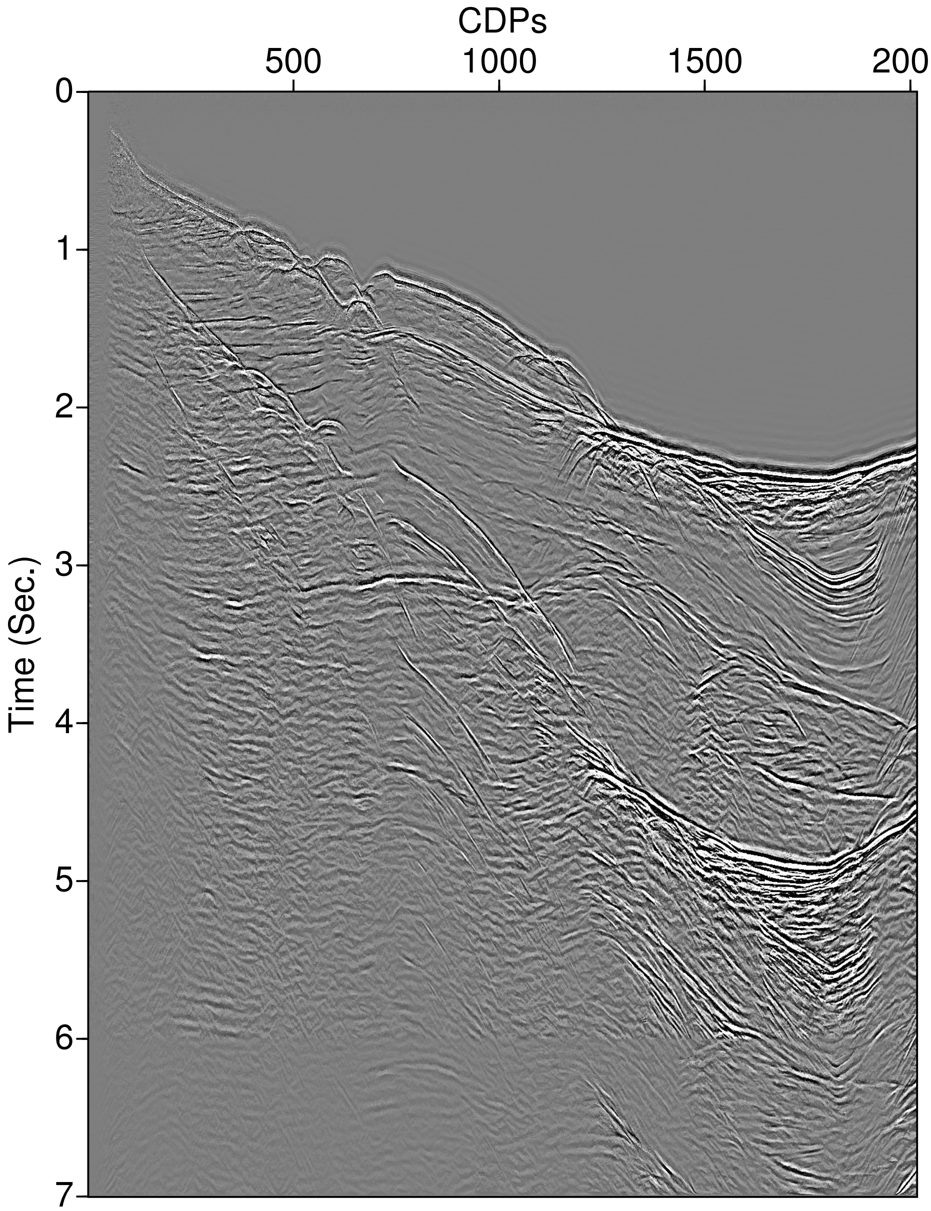

Figure 5: CRS stack result for the real marine data set without smoothing of CRS parameters.

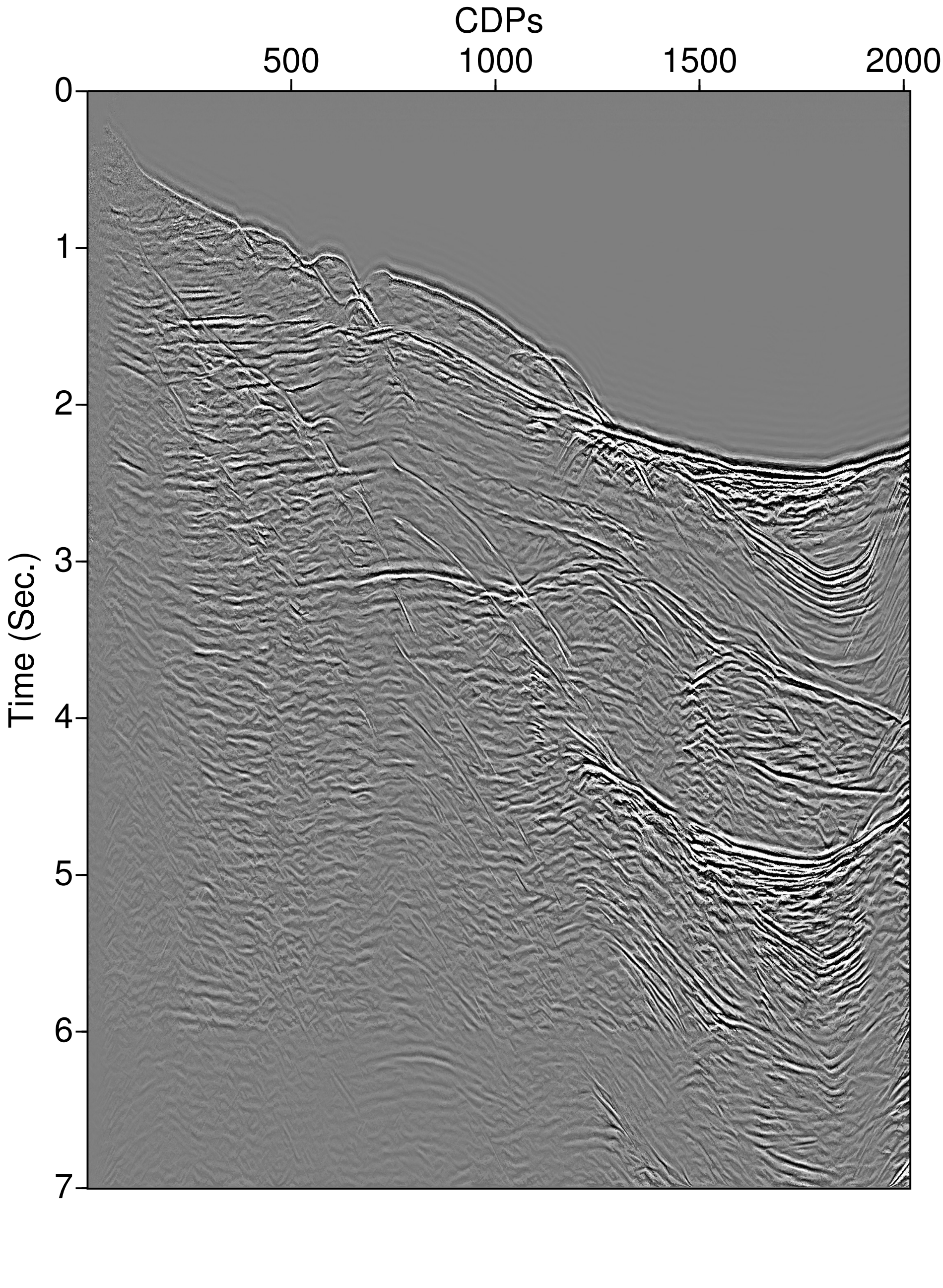

Figure 6: CRS stack result for the real marine data set with smoothed CRS parameters β_0 and K_{NIP}.

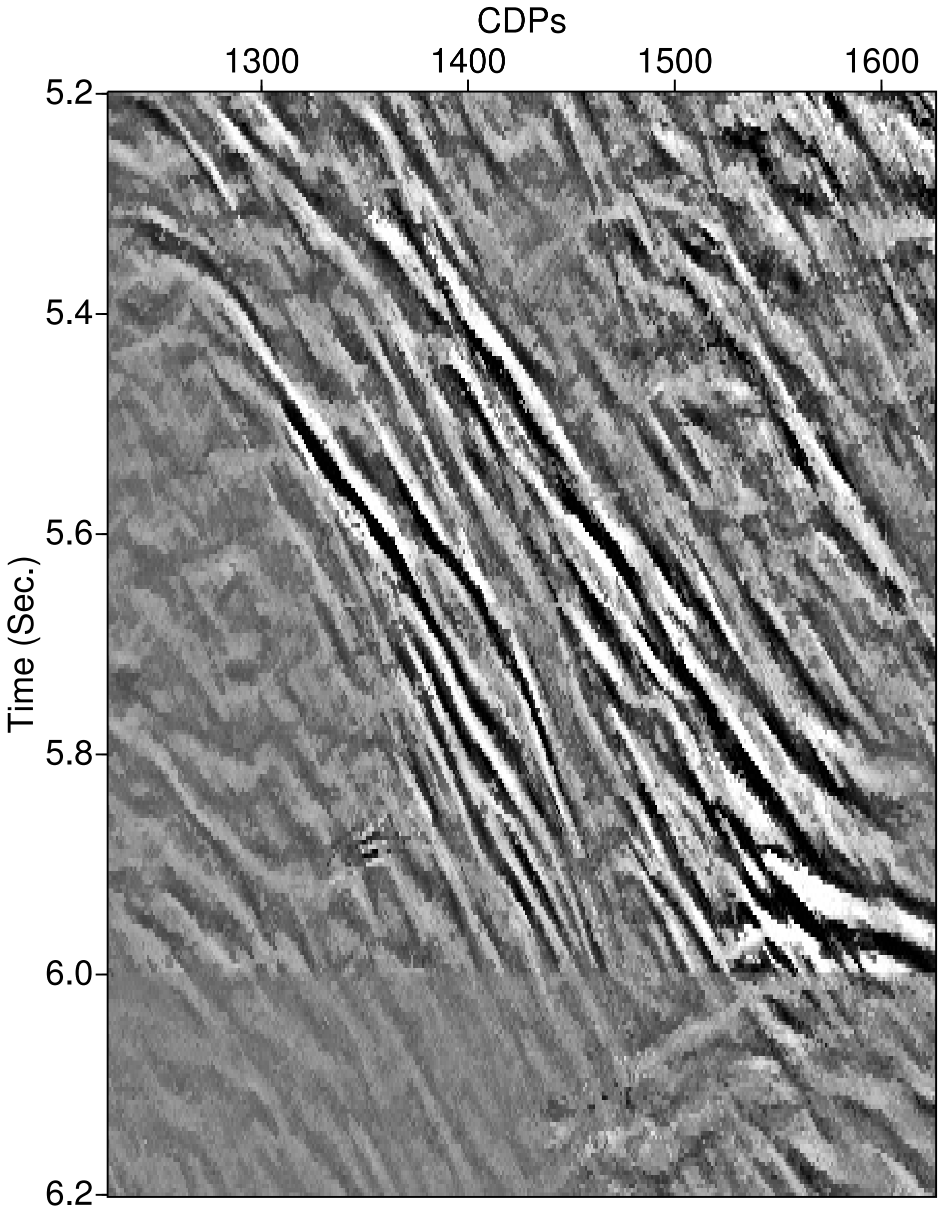

Figure 7: Detail from the CRS stack result for the real marine data set without parameter smoothing.

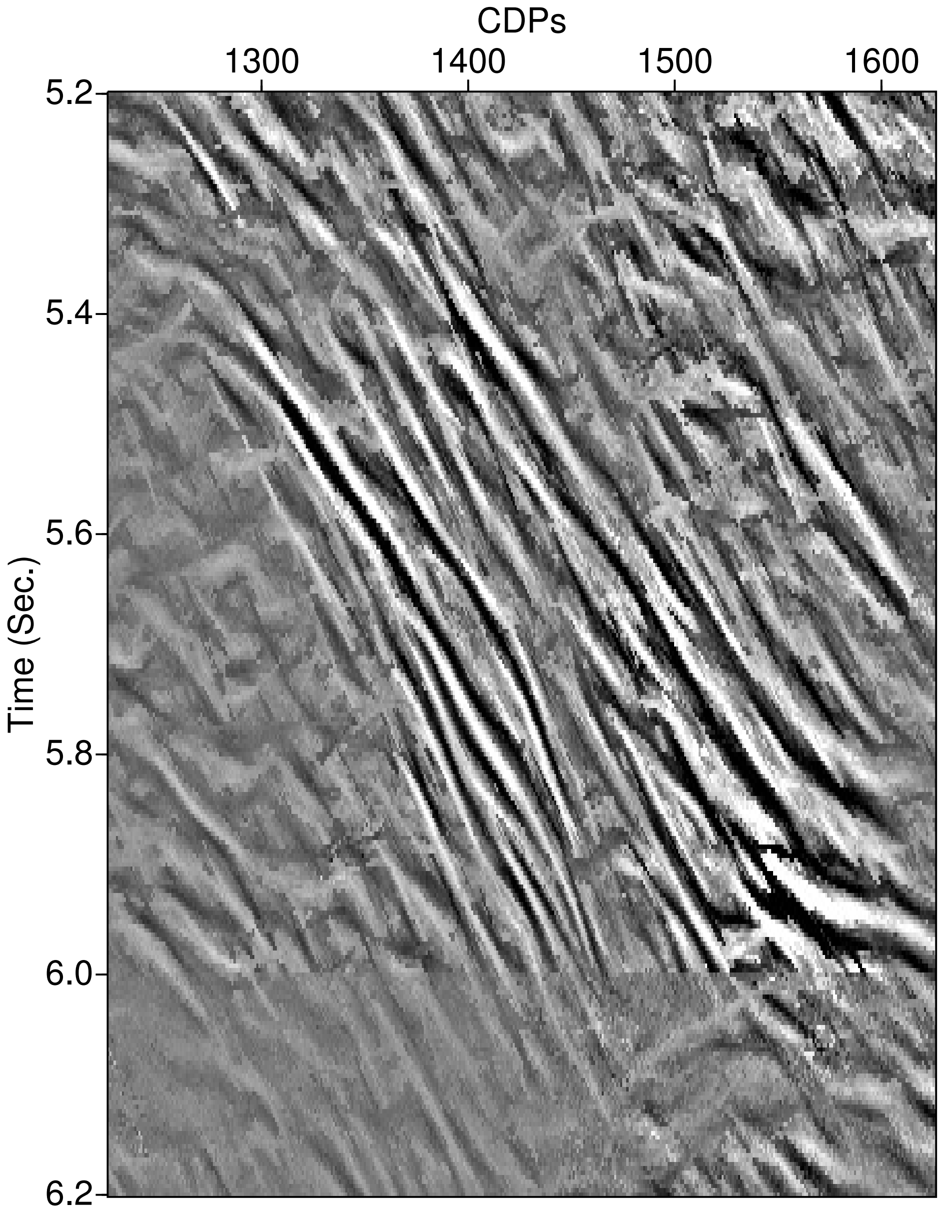

Figure 8: Same detail from the CRS stack as in Figure 7 with smoothed β_0 and K_{NIP}.

Mi, Y. and Margrave, G. F. (2000). Median filtering in kirchhoff migration for noisy data. In *Expanded Abstracts, 70th Ann. Internat. Mtg.*, pages 822–825. Soc. Expl. Geophys.

Neelamani, R., Baumstein, A. I., Gillard, D. G., Hadidi, M. T., and Soroka, W. I. (2008). Coherent and random noise attenuation using the curvelet transform. *The Leading Edge*, 27:240–248.

Ristau, J. P. and Moon, W. M. (2001). Adaptive filtering of random noise in 2-D geophysical data. *Geophysics*, 66:342–349.

Yilmaz, O. (2001). *Seismic Data Analysis, Vols. 1 and 2*. Soc. Expl. Geophys.